Nanoscale

PAPER

View Article Online
View Journal | View Issue

Cite this: *Nanoscale*, 2023, **15**, 10749

Histidine–DNA nanoarchitecture as laccase mimetic DNAzymes†

Ji Hye Yum,[a] Tomotaka Kumagai,[a] Daisuke Hori,[a] Hiroshi Sugiyama *[a,b] and Soyoung Park *[c]

Received 8th April 2023,
Accepted 10th June 2023

DOI: 10.1039/d3nr01625k

rsc.li/nanoscale

Herein, we report on the construction of Cu–histidine (**His**)–DNA hybrids as laccase-mimetic DNAzymes. Cu–**His**–DNAzymes showed remarkable activity in a colorimetric oxidation reaction between 2,4-dichlorophenol and 4-aminoantipyrine. Our results provide new insights for the systematic construction of tailor-made active sites for biomimetics.

Introduction

Nucleic acids have received immense attention as versatile biomaterials that can play several roles across the various sciences.[1] They offer many advantages, including automated chemical synthesis, thermal stability, programmability, and creation of a diverse range of tertiary structures constructed from hydrogen bonding between the four bases (*i.e.*, A, T/U, G, C). By leveraging these intrinsic features, DNA nanotechnology has made momentous advances in chemical biology, materials science, medicinal chemistry, and pharmacology.[2] In addition, recent studies have demonstrated the previously unnoticed function of DNA as a bioscaffold for catalysis.[3] These papers have reported the versatility of DNA-based hybrid catalysts for various chemical reactions, such as Diels–Alder reactions, Friedel–Crafts alkylation, and Michael addition.[4] In addition, the chemical modification of native nucleic acids with various functional moieties has facilitated further improvements to their capability. These functional moieties can be sequence-specifically implemented on nucleic acid strands due to advances in phosphoramidite chemistry and solid-phase DNA synthesis.[5] These pioneering works on DNA/RNA modification with ligands, fluorophores, and the precursors of biorthogonal reactions have created an opportunity for modulating molecular machinery using synthetic oligonucleotides.[6] Amino acid residues are very promising building blocks for modifying DNA oligonucleotides because they are abundant natural materials that display diverse functional characteristics.[7] By hybridizing amino acid residues with oligonucleotides, the utility and effectiveness of nucleic acids can be reinforced. For instance, the conjugation of cationic polypeptides to nucleic acid-based therapeutic drugs led to charge-neutralization and thus improved cellular uptake efficiency.[8] Nucleopeptides have also been widely used as a unit for fabricating supramolecular nanocarriers, fibers, and hydrogels through alternative hydrogen bond formation between amino acid side chains and nucleotides.[9] Due to the broad potential of biomedical and industrial applications, a handy and straightforward approach is required to synthesize amino acids-conjugated oligonucleotides. Our group has been involved in the development of modified oligonucleotides and has established a systematic strategy to incorporate amino acid residues into oligonucleotides *via* a D-threoninol linker.[10] We have named these amino acid-conjugated DNA as amino acid–nucleic acid hybrids (ANHs). In a previous study we synthesized histidine-conjugated DNA oligonucleotides and demonstrated their capability as metal reservoirs. Histidine-containing DNA (**His**–DNA) was successfully used as an asymmetric catalyst for Diels–Alder reactions. **His**–DNA–hemin complexes showed remarkable catalytic performance in 2,2′-azino-bis(3-ethylbenzothiazoline-6-sulfonic acid) oxidation. We have further exploited ANHs to construct an advanced aptamer library as a post-SELEX modification approach. We have generated amino acid-functionalized thrombin-binding aptamers and successfully demonstrated their utility with enhancement of thrombin inhibition activity and nuclease resistance.[11] Encouraged by the remarkable performance of ANHs, we have moved forward to the goal of exploiting ANHs that can mimic enzymes by the construction of active sites on DNA strands with key amino acids. Laccase is a class of phenol oxidases widely applied in environmental remediation by catalyzing the oxidation of toxic phenols and amines.[12] Because laccase reactions use molecular oxygen as the electron acceptor to release water without the production

[a]*Department of Chemistry, Graduate School of Science, Kyoto University, Kitashirakawa-oiwakecho, Sakyo-ku, Kyoto 606-8502, Japan*
[b]*Institute for Integrated Cell-Material Sciences (iCeMS), Kyoto University, Yoshida-ushinomiyacho, Sakyo-ku, Kyoto 606-8501, Japan*
[c]*Immunology Frontier Research Center, Osaka University, Yamadaoka, Suita, Osaka, 565-0871, Japan. E-mail: spark@ifrec.osaka-u.ac.jp*

† Electronic supplementary information (ESI) available. See DOI: https://doi.org/10.1039/d3nr01625k

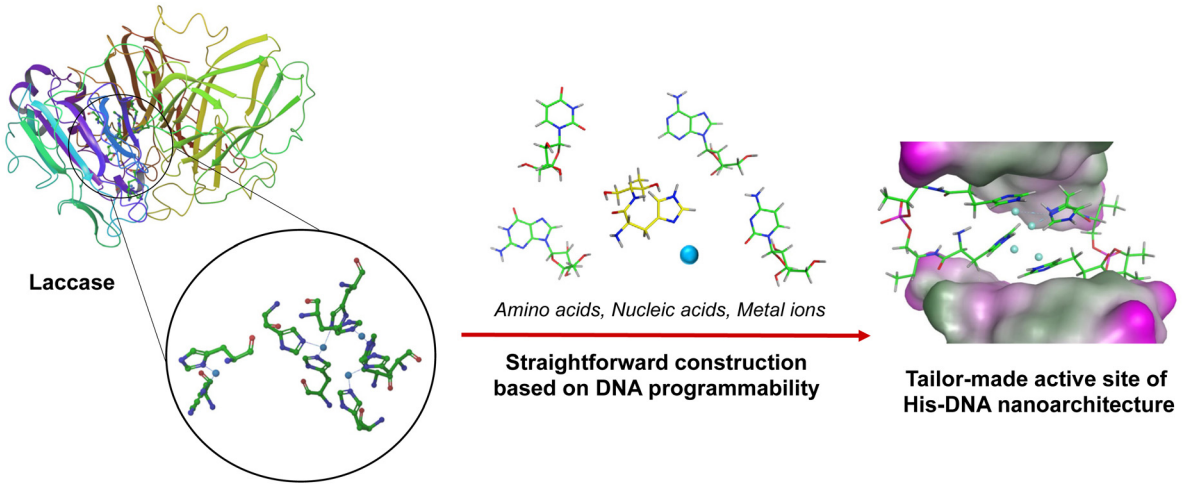

Fig. 1 A laccase-mimetic Cu–**His**–DNAzyme containing multiple histidine residues in the active sites.

of hydrogen peroxide, the use of laccase is attracting attention in terms of "green" catalysis. This has led to efforts toward the development of laccase-mimetic materials.[16]

For instance, enzyme immobilization and directed evolution have been explored to overcome vulnerable aspects of natural enzymes, and metal–organic framework-based nanozymes were reported to expand applications of laccase.[13,17] In the active site of laccase, four copper ions are coordinated with multiple histidine residues. We postulated a rational design for a laccase-mimetic apoenzyme by incorporating histidine residue on the various DNA structures. It would be activated as the holoenzyme for catalysis *via* the coordination of copper ions (Fig. 1). Here we report on the construction of advanced Cu–histidine (**His**)–DNA hybrids as laccase-mimetic DNAzymes and their catalytic performance in a standard colorimetric oxidation reaction between 2,4-dichlorophenol and 4-aminoantipyrine (Scheme 1).

Results and discussion

A series of DNA metalloenzymes functionalized with **His** residues were designed based on the copper-coordinated histidine-rich catalytic domain of laccase (PDB ID: 2X88). A threoninol-tethered histidine residue was synthesized as reported previously.[10,11] To construct an active site capable of coordinating multiple copper ions, **His**-containing phosphoramidites were sequence-specifically installed on oligonucleotides through automated solid-phase DNA synthesis (Scheme 2). **His**-modified DNAs with palindromic sequences (5′-GGACC-**His**-**His**-GGTCC-3′) were obtained in high yield (overall synthetic yields ~70%) after the consecutive incorporation of **His** modules. Together with canonical B-DNA, diverse tertiary DNA structures including a G-quadruplex, a quadruplex–duplex hybrid, and three-way junction (3WJ) DNAs were designed as scaffolds for **His** functionalization (Table S1†). All oligomers were purified through reverse HPLC and then identified using MALDI-TOF-MS spectroscopy. Circular dichroism (CD) analysis provides structural information on DNA, and we confirmed that the **His**-functionalized oligomers possessed the desired conformations (Fig. S1†). Besides canonical B-helical structures of duplex–**HH** and 3WJ–**HH**, interG4–**HH** was characterized as an intermolecular parallel G-quadruplex in potassium ion solution. We also observed the antiparallel G-quadruplex of QD–**HH** in the presence of potassium. To investigate the

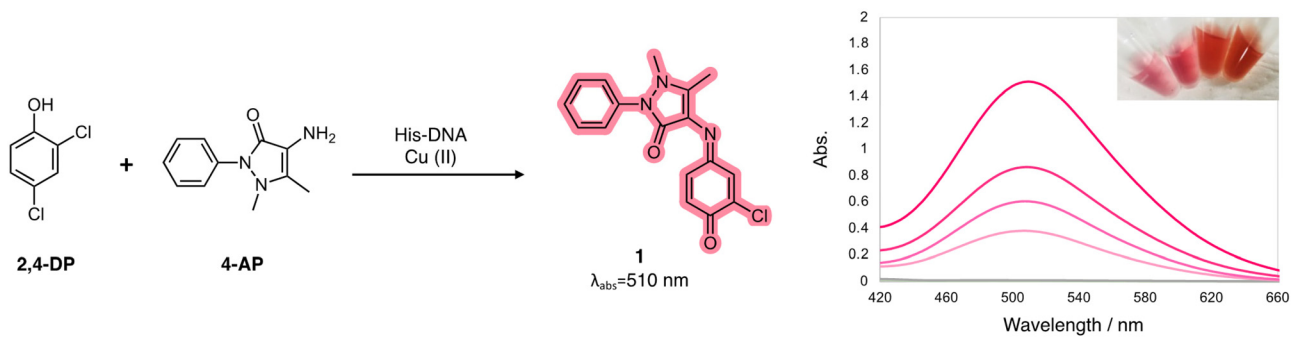

Scheme 1 Colorimetric oxidation reaction between phenolic compound **1** and aromatic amine **2** catalyzed by laccase-mimetic Cu–**His**–DNAzymes.

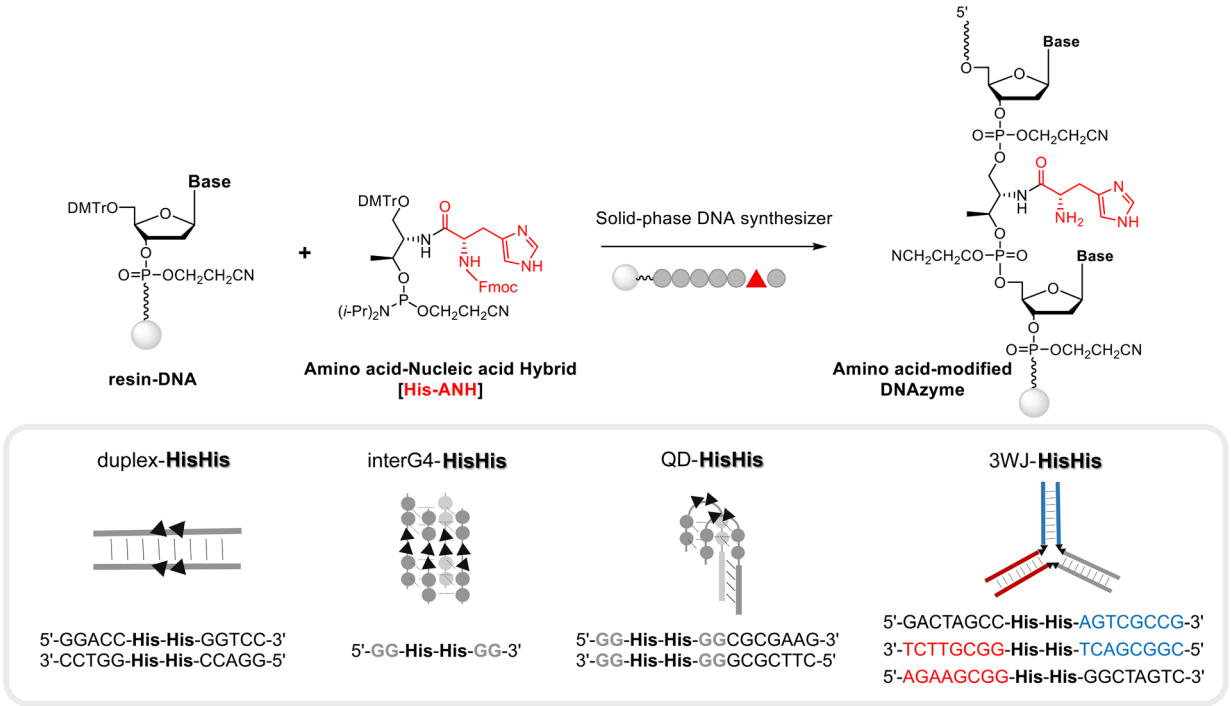

Scheme 2 Modular strategy for constructing a library of amino acid-modified DNAzymes *via* solid-phase DNA synthesis (for the synthesis details and identification of various DNAzymes, please see the ESI†).

thermal stability of the novel **His**–DNA hybrids, we measured melting temperatures (T_m) in the absence and presence of Cu(II) ions (Fig. S2†). For both duplex–**HH** and interG4–**HH**, we observed significant increases in T_m values in the presence of Cu(II) ions (ΔT_m = 6.8 °C and 2.5 °C, respectively). For QD–**HH**, a remarkable thermal stabilization effect (ΔT_m = 14.6 °C) was observed on the addition of Cu(II) ions. Considering the structural characterization through spectroscopy, computational modelling was done to gain further insight into the structural motifs of the **His**–DNA nanostructures. The plausible structures of **His**–DNA hybrids were simulated with reported PDB structures and CHARM force-field parameters. As shown in Fig. S6–S9,† the energetically minimized structures suggest well-constructed microenvironments for metal–histidine coordination in the designed active sites. Next, we proceeded to validate the catalytic ability of **His**–DNA metalloenzymes as multicopper oxidases. The oxidation of 2,4-dichlorophenol (2,4-DP) and 4-aminoantipyrine (4-AP) was chosen as the model reaction (Scheme 1). A **His**–DNA-based catalysis system was thus constructed by mixing **His**–DNAs and various equivalents of $Cu(NO_3)_2$ in 20 mM MOPS buffer (pH 7.0) with 100 mM NaCl. Substrates 2,4-DP and 4-AP were then added to the **His**–DNA solution such that the final catalyst loading was 0.1 mol% for duplex DNA and 0.1–1.0 mol% for the catalytic metal. Because product 1 absorbs visible light (510 nm, magenta, Fig. S5†), the reaction progress was quantified through absorption spectroscopy (Fig. 2A and B). The rapid increase of the absorption intensity at 510 nm indicated that **His**-functionalized DNAzymes were able to catalyze the reaction. The reaction plateaued after 12 h (Fig. S3B†). We then explored other transition metals to investigate whether they were able to catalyze the phenol oxidation reaction (Fig. S4†). However, none of them resulted in an absorption band at 510 nm. The use of DNA in the absence of Cu(II) did not afford an absorption band of target product 1 (data not shown). This suggests that Cu(II) ions is necessary for the present reaction. We examined the reactivity of duplex–**HH** DNA with various Cu(II) ion concentrations (Fig. 2B). We found that the reactivity of Cu–**His**–DNAzymes increased significantly as the concentration of Cu(II) ions increased and exhibited comparable catalytic performance to that of laccase even under low Cu(II) ion (0.1 mol%) concentrations. We settled on 1.0 mol% Cu(II) ions and 0.1 mol%-modified oligomers as optimized conditions for further investigation. In a previous study, we observed that the catalytic performance of DNA-based hybrid catalysts varied depending on the tertiary structures of DNA.[14] For instance, a duplex-based DNA hybrid catalyst showed very low reactivity in the asymmetric Michael addition reaction, whereas a G-quadruplex DNA hybrid catalyst resulted in excellent yield and stereoselectivity. Accordingly, we conducted the laccase-mediated oxidation reaction with various Cu–**His**–DNAzymes and found that DNA structures significantly affected the reaction progress (Fig. 2C). InterG4–**HH** DNA constructed with a four-stranded parallel quadruplex bearing 8 **His** modules for the catalytic pocket significantly promoted the oxidation reaction as reported by previous studies based on G-quadruplex-mediated catalytic systems.[18] In addition, kinetic parameters including V_{max}, k_{cat} and K_m could be calculated by Michaelis–

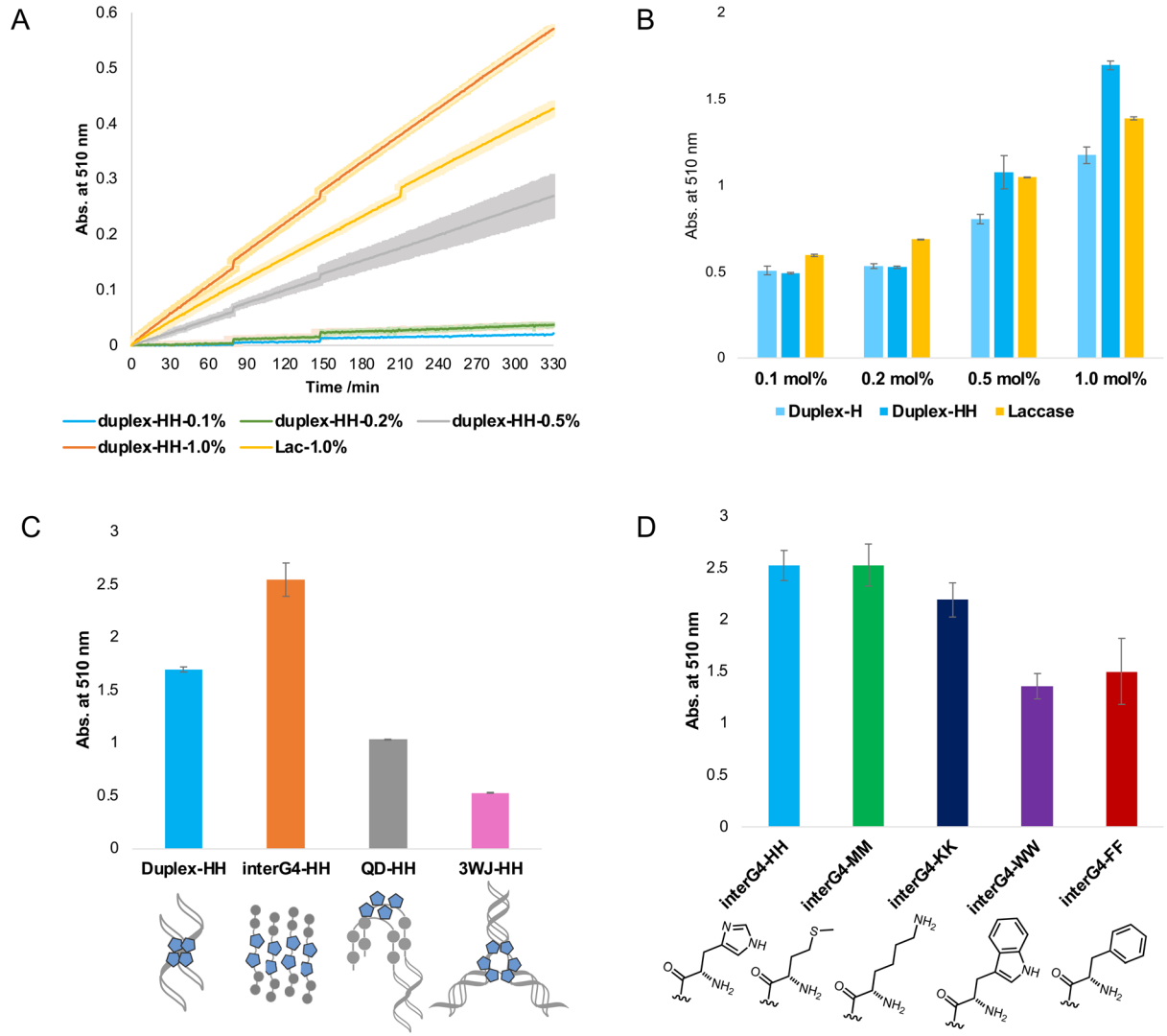

Fig. 2 Catalytic performance of laccase-mimetic Cu–**His**–DNAzymes for oxidation reactions. (A) Absorption spectra of the reaction progress (5.5 h). (B) Activity comparison under various copper ion concentration after the reaction for 12 h. (C) Activity comparison catalyzed by **His**–DNA with various secondary structures. (D) Activity comparison with inter-G4-containing various ANH modules. All reactions were performed in triplicate.

Menten equation (Table S2†). Based on the analysis of kinetic parameters, it was observed that Cu–**His**–DNAzymes exhibited significant catalytic efficiency (k_{cat}/K_m) compared to laccase under the given reaction conditions. A better binding affinity (K_m) was observed with interG4–**HH** DNA and duplex–**HH** DNA afforded a higher turnover number (k_{cat}). A three-way junction DNA (3WJ–**HH**) showed relatively lower catalytic activities that other catalysts. These results indicate that the microenvironment of active site generated by DNA tertiary structures could determine the capability of ANH-based DNAzymes. Subsequently, we asked whether the incorporation of other amino acid residues could mediate the oxidation reaction as laccase mimics. Thus, we introduced four different ANH modules (*i.e.*, Lys, Met, Trp, and a Phe), into the concise intermolecular G-quadruplex-forming DNA sequences (Scheme S1†). DNA was found to be functionalized with aromatic amino acids (*i.e.*, Trp and Phe), which gave lower yields of the chromogenic product. In contrast, DNA functionalized with amino acids that enabled metal ion coordination (*i.e.*, Met- and Lys-containing intermolecular G-quadruplexes) displayed similar catalytic ability to **His**–DNAs. The results for Met-modified DNA are particularly noteworthy in that methionine participates in Cu(II) coordination in the catalytic pocket and provides catalytic performance as a novel laccase surrogate. This suggests that ANH-based DNAzymes can exhibit native enzyme-like behaviour by the combination of suitable amino acid residues in oligonucleotides. Further, the catalytic performances of the present modular DNAzymes can be further improved through the optimization of DNA structures and amino acid residues as demonstrated above.

Conclusions

In conclusion, we developed a laccase mimic using a DNA scaffold with minimal amino acid componentry. The Cu–**His**–DNAzyme activity was modulated their catalytic performance with various design features such as DNA tertiary structures and DNA/amino acid sequences. Our results demonstrate the potential of rationally designed DNAzymes as an alternative strategy to protein-based enzymes and inorganic nanozymes:[15] (1) DNAzymes are biodegradable, biohybrid catalysts that are harmless to the environment; (2) they are highly versatile because their spatial structure and the capability as metal deposit can be modulated; (3) the molar mass of our DNAzyme is *ca.* 7.3 kDa, spanning 20 nm, which is remarkably compact compared with the native protein (Trametes Versicolor laccase, 22 kDa) and Cu-GMP nanozyme (particle size, about 1500 nm).[13f] By employing a straightforward technology, tailor-made active sites could be systematically designed and constructed with ANH modules. We hope the present study will trigger new insights in a variety of research fields and inspire the further application of an ANH modular assembly for biomimetics.

Author contributions

Soyoung Park (S. P.) and Ji Hye Yum (J. H. Y.) conceptualized and designed research. J. H. Y. carried out the synthesis and characterization of the compounds and analyzed the data. Tomotaka Kumagai (T. K.) and Daisuke Hori (D. H) validated the data. S. P. and J. H. Y. wrote original draft. S. P., D. H. and T. K. edited the manuscript. S. P. and Hiroshi Sugiyama (H. S.) supervised the project and reviewed the manuscript. S. P. and H. S. acquired the research funding and provided resources.

Conflicts of interest

The authors declare no competing financial interest.

Acknowledgements

We would like to thank Karin Nishimura (Graduate School of Engineering, Kyoto University) for technical assistance in obtaining the mass spectra of synthesized compounds. S. P. appreciate the financial support by Grant-in-Aid for Transformative Research Area (A) [23H04076; "Material Symbiosis"]. This work was also supported by AMED under 22ama121025j0001 (Platform Project for Supporting Drug Discovery and Life Science Research (BINDS)) to S. P. and JSPS 20H05936 and 21H04705 to H. S.

References

1 (*a*) N. C. Seeman, *Nature*, 2003, **421**, 427; (*b*) S. M. Douglas, H. Dietz, T. Liedl, B. Högberg, F. Graf and W. M. Shih, *Nature*, 2009, **459**, 414.

2 (*a*) M. Zahid, B. Kim, R. Hussain, R. Amin and S. H. Park, *Nanoscale Res. Lett.*, 2013, **8**, 1; (*b*) Y. Ke, C. Castro and J. H. Choi, *Annu. Rev. Biomed. Eng.*, 2018, **20**, 375; (*c*) J. L. Mergny and D. Sen, *Chem. Rev.*, 2019, **119**, 6290.

3 (*a*) S. Park and H. Sugiyama, *Angew. Chem., Int. Ed.*, 2010, **49**, 3870; (*b*) A. Rioz-Martínez and G. Roelfes, *Curr. Opin. Chem. Biol.*, 2015, **25**, 80; (*c*) S. Park and H. Sugiyama, *Molecules*, 2012, **17**, 12792; (*d*) S. K. Silverman, *Trends Biochem. Sci.*, 2016, **41**, 595; (*e*) N. Duchemin, I. Heath-Apostolopoulos, M. Smietana and S. Arseniyadis, *Org. Biomol. Chem.*, 2017, **15**, 7072; (*f*) J. H. Yum, S. Park and H. Sugiyama, *Org. Biomol. Chem.*, 2019, **17**, 9547; (*g*) J. H. Yum, H. Sugiyama and S. Park, *Chem. Rec*, 2022, e202100333.

4 (*a*) S. Park, K. Ikehata, R. Watabe, Y. Hidaka, A. Rajendran and H. Sugiyama, *Chem. Commun.*, 2012, **48**, 10398; (*b*) S. Park, L. Zheng, S. Kumakiri, S. Sakashita, H. Otomo, K. Ikehata and H. Sugiyama, *ACS Catal.*, 2014, **4**, 4070; (*c*) S. Park, I. Okamura, S. Sakashita, J. H. Yum, A. Chiranjit, L. Gao and H. Sugiyama, *ACS Catal.*, 2015, **5**, 4708; (*d*) J. H. Yum, S. Park, R. Hiraga, I. Okamura, S. Notsu and H. Sugiyama, *Org. Biomol. Chem.*, 2019, **17**, 2548.

5 W. Bannwarth, *Helv. Chim. Acta*, 1988, **71**, 1517.

6 (*a*) N. S. Oltra and G. Roelfes, *Chem. Commun.*, 2008, 6039; (*b*) W. Xu, K. M. Chan and E. T. Kool, *Nat. Chem.*, 2017, **9**, 1043; (*c*) A. H. El-Sagheer and T. Brown, *Chem. Soc. Rev.*, 2010, **39**, 1388.

7 (*a*) M. Sarikaya, C. Tamerler, A. K.-Y. Jen, K. Schulten and F. Baneyx, *Nat. Mater.*, 2003, **2**, 577; (*b*) M. Sato and T. J. Webster, *Expert Rev. Med. Devices*, 2004, **1**, 105.

8 P. Geotti-Bianchini, J. Beyrath, O. Chaloin, F. Formaggio and A. Bianco, *Org. Biomol. Chem.*, 2008, **6**, 3661.

9 (*a*) K. Baek, A. D. Noblett, P. Ren and L. J. Suggs, *ACS Appl. Bio Mater.*, 2019, **2**, 2812; (*b*) S. Fleming and R. V. Ulijn, *Chem. Soc. Rev.*, 2014, **43**, 8150; (*c*) F. Gelain, A. Horii and S. Zhang, *Macromol. Biosci.*, 2007, **7**, 544.

10 S. Park, H. Matsui, K. Fukumoto, J. H. Yum and H. Sugiyama, *RSC Adv.*, 2020, **10**, 9717.

11 J. H. Yum, T. Ishizuka, K. Fukumoto, D. Hori, H.-L. Bao, Y. Xu, H. Sugiyama and S. Park, *ACS Biomater. Sci. Eng.*, 2021, **7**, 1338.

12 (*a*) P. Giardina, V. Faraco, C. Pezzella, A. Piscitelli, S. Vanhulle and G. Sannia, *Cell. Mol. Life Sci.*, 2010, **67**, 369; (*b*) J.-R. Jeon, P. Baldrian, K. Murugesan and Y.-S. Chang, *Microb. Biotechnol.*, 2012, **5**, 318; (*c*) C. Galli, C. Madzak, R. Vadalà, C. Jolivalt and P. Gentili, *ChemBioChem*, 2013, **14**, 2500; (*d*) B. Ghosh, R. Saha, D. Bhattacharya and M. Mukhopadhyay, *Bioresour. Technol. Rep.*, 2019, **6**, 268; (*e*) A. D. Moreno, D. Ibarra, M. E. Eugenio and E. Tomas-Pejo, *J. Chem. Technol. Biotechnol.*, 2020, **95**, 481.

13 (*a*) S. K. S. Patel, H. Choi and J.-K. Lee, *ACS Sustainable Chem. Eng.*, 2019, **7**, 13633; (*b*) L. Zhang, W. Tang, T. Ma, L. Zhou, C. Hui, X. Wang, P. Wang, C. Zhang and C. Chen, *RSC Adv.*, 2019, **9**, 38935; (*c*) L. Zhang, H. Cui, Z. Zou, T. M. Garakani, C. Novoa-Henriquez, B. Jooyeh and

U. Schwaneberg, *Angew. Chem., Int. Ed.*, 2019, **58**, 4562; (*d*) M. A. Molina, J. Díez-Jaén, M. Sánchez-Sánchez and R. M. Blanco, *Catal. Today*, 2022, **390–391**, 265; (*e*) S. Patra, S. Sene, C. Mousty, C. Serre, A. Chaussé, L. Legrand and N. Steunou, *ACS Appl. Mater. Interfaces*, 2016, **8**, 20012; (*f*) H. Liang, F. Lin, Z. Zhang, B. Liu, S. Jiang, Q. Yuan and J. Liu, *ACS Appl. Mater. Interfaces*, 2017, **9**, 1352.

14 J. H. Yum, H. Sugiyama and S. Park, *Org. Biomol. Chem.*, 2020, **18**, 6812.

15 (*a*) H. Liang, F. Lin, Z. Zhang, B. Liu, S. Jiang, Q. Yuan and J. Liu, *ACS Appl. Mater. Interfaces*, 2017, **9**, 1352; (*b*) J. Wu, X. Wang, Q. Wang, Z. Lou, S. Li, Y. Zhu, L. Qin and H. Wei, *Chem. Soc. Rev.*, 2018, **48**, 1004; (*c*) D. Jiang, D. Ni, Z. T. Rosenkrans, P. Huang, X. Yan and W. Cai, *Chem. Soc. Rev.*, 2019, **48**, 3683; (*d*) Y. Huang, J. Ren and X. Qu, *Chem. Rev.*, 2019, **119**, 4357–4412; (*e*) X. Xu, J. Wang, R. Huang, W. Qi, R. Su and Z. He, *Catal. Sci. Technol.*, 2021, **11**, 3402.

16 (*a*) J. Yang, W. Li, T. B. Ng, X. Deng, J. Lin and X. Ye, *Front. Microbiol.*, 2017, **8**, 832; (*b*) T. Brugnari, D. M. Braga, C. S. A. Santos, B. H. C. Torres, T. A. Modkovski, C. W. I. Haminiuk and G. M. Maciel, *Bioresour. Bioprocess*, 2021, **8**, 131; (*c*) I. Bassanini, E. E. Ferrandi, S. Riva and D. Monti, *Catalysts*, 2021, **11**, 26; (*d*) L. Lei, X. Yang, Y. Song, H. Huang and Y. Li, *New J. Chem.*, 2022, **46**, 3541.

17 (*a*) J. Wang, R. Huang, W. Qia, R. Sua, B. P. Binks and Z. He, *Appl. Catal., B*, 2019, **254**, 452; (*b*) S. Shams, W. Ahmad, A. H. Memon, Y. Wei, Q. Yuan and H. Liang, *RSC Adv.*, 2019, **9**, 40845; (*c*) A. Koyappayil, H. T. Kim and M.-H. Lee, *J. Hazard. Mater.*, 2021, **412**, 125211; (*d*) R. Su and Z. He, *Catal. Sci. Technol.*, 2021, **11**, 3402; (*e*) L. Huang, Y. Tang, J. Wang, X. Niu, J. Zhou and Y. Wu, *Sens. Actuators, B*, 2023, **391**, 134052.

18 (*a*) E. Golub, H. B. Albada, W.-C. Liao, Y. Biniuri and I. Willner, *J. Am. Chem. Soc.*, 2016, **138**, 164; (*b*) H. B. Albada, J. W. Vries, Q. Liu, E. Golub, N. Klement, A. Herrmann and I. Willner, *Chem. Commun.*, 2016, **52**, 5561; (*c*) H. B. Albada, E. Golub and I. Willner, *Chem. Sci.*, 2016, **7**, 3092; (*d*) J. Chen, Y. Zhang, M. Cheng, Y. Guo, J. Šponer, D. Monchaud, J.-L. Mergny, H. Ju and J. Zhou, *ACS Catal.*, 2018, **8**, 11352; (*e*) P. M. Punt and G. H. Clever, *Chem. Sci.*, 2019, **10**, 2513; (*f*) P. M. Punt and G. H. Clever, *Chem. – Eur. J.*, 2019, **25**, 13987.